Notas e Resenhas

REFINEMENT OF THE DIGITAL ELEVATION MODEL APPLIED TO EROSION MODELING OF WATERSHEDS

INTRODUCTION

Rapid soil erosion is a major threat to the sustainability of ecosystems (PIMENTEL et al., 1995, p.1118). The increase in erosion processes across the Alto Taquari sub-basin (BAT) intensified silting up the Taquari river in the Pantanal region, and consequently the inundation of floodplain areas around its lower course. This inundation is considered the most severe impact, both environmentally and socio-economically for the Pantanal (GALDINO; PELLEGRIN, 2003, p.11).

Among all sub-basins within the Alto Paraguai watershed (BAP), BAT is one of the regions showing the highest erosion potential (GALDINO et al., 2006, p.113), and also one of the highest rates of sediment production (GALDINO; PELLEGRIN, 2003, p.23). Therefore, a modeling of erosion processes aiming to reduce the amount of sediment is a necessity presented for the conservation plan of BAP, also applied to BAT (GALDINO; PELLEGRIN, 2003, p.26). In the context, erosion modeling allows an evaluation of the erosion potential of natural and human factors, thus supporting the conservation plan of that watershed (BOTELHO, 2009, p.277).

The empiric model named Universal Soil Loss Equation (USLE) (WISCHMEIER; SMITH, 1978, p.4) allows the estimation of soil loss caused by hydric erosion in a given area which was originally an agricultural field.

This model is described by the equation: $A = R \ x \ K \ x \ L \ x \ S \ x \ C \ x \ P$. Where A (t.ha^{-1}.year^{-1}) equals the average amount of soil lost in a given area during a certain period of time; R (MJ.mm.ha^{-1}. h^{-1}.year^{-1}) is the Rainfall erosivity factor; K (t.h.MJ^{-1}.mm^{-1}) stands for soil erodibility; $L \ x \ S$ corresponds to the topographic factor; and C and P are respectively the factors which consider land use and soil conservation practices.

Presently with the availability of the Geographic Information Systems (SIG), the USLE model is applied to erosion modeling in large areas, thus allowing to analyze the characteristics of the physical environment from BAT and its natural potential for erosion (GALDINO et al., 2006, p.107). However, the original concept of LS topographic factor does not consider interactions between the runoff of the surface flow, which is the main eroding agent, and the relief forms in the area analyzed, typically a watershed.

The topographic factor used in the USLE model considers the influence of slope length (λ) and slope angle (θ) on erosion processes to calculate respectively factors L and S. However the ratio between potential for erosion and slope length is genuinely empirical, lacking a physical foundation and a theoretical basis to justify it (MOORE; BURCH, 1986, p.1294).

So the two-dimensional topographic factor ($LS2d$) differentiated by the substitution of slope length λ with unit contributing area (As), allows to combine the influence of relief forms from a watershed on the superficial runoff flow in the modeling of erosion processes (MOORE; BURCH, 1986, p.1295). Figure 1 illustrates the differences between the topographic variables slope length λ and unit contributing area As as it is used in the calculation of the topographic factor LS, and the two-dimensional topographic factor $LS2d$, respectively.
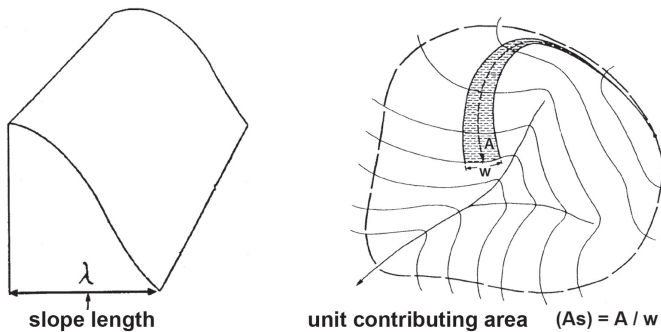
Figure 1 - Representation of the topographic variables slope length (λ), slope angle (θ) and unit contributing area (As) employed in calculation of topographic factor (LS) and two-dimensional topographic factor ($LS2d$)

$LS2d$ can be estimated based on the digital elevation model (DEM) calculating the contributing area ($A_{(i,j)}$), slope ($\theta_{(i,j)}$), and aspect ($\phi_{(i,j)}$) in a given DEM cell located on row i and column j. Topographic variables $\theta_{(i,j)}$ and $\phi_{(i,j)}$ can be calculated from neighborhood relations of DEM cells (ZEVENBERGEN; THORNE, 1987). The variable $A_{(i,j)}$ may be calculated using routing algorithms, and the most cited in literature are: Deterministic 8 (O'CALLAGHAN; MARK, 1984), Multiple Flow Direction (FREEMAN, 1991; QUINN et al., 1991), Flux Decomposition (DESMET; GOVERS, 1996b), and Deterministic Infinity (TARBOTON, 1997).

So the potential for erosion relative to topographic characteristics can be calculated based on the relief structure as described by DEM. This approach enables the identification of areas vulnerable to erosion based on the characteristics of the runoff surface flow, which are conditioned by watershed relief (DESMET; GOVERS, 1996a, p.431).

The use of a hydrologically consistent topographic factor (calculated on the estimated surface flow) to model erosion in watersheds according to DEM, is a key to permit the analysis of the spatial distribution of sediments produced in the erosion process (KINNEL, 2005, p.679). Therefore, calculating the $LS2d$ factor based on DEMs originated from the Shuttle Radar Topography Mission (SRTM) data can help to assess the potential for erosion relative to topographic characteristics of a watershed (VERSTRAETEN, 2006, p.138).

In order to improve evaluation of the spatial erosion distribution in watersheds that affect the biome from the Pantanal, it is necessary to understand how the characteristics of DEM may influence the identification of areas most susceptible to water erosion. Within this context, the objective of this study is to evaluate the influence of the refinement from the digital elevation model on the calculation of $LS2d$, a factor used to model erosion in watersheds. We verified the implications resulting from variations of the grid spacing from the DEM, to identify areas with topographic characteristics which are most susceptible to erosion processes, in an experimental small catchment.

CHARACTERIZING THE AREA UNDER STUDY

The area under study (figure 2) is the Córrego do Veado sub-basin, located in the municipality of Coxim (MS), and it was selected because its topographic variety is adequate for the purpose of this research. The Córrego do Veado sub-basin is part of BAT, and therefore located within BAP. It got code 895634 under the ottobasin classification adopted by the Brazilian National Agency for Water (Agência Nacional de Águas – ANA, 2010).
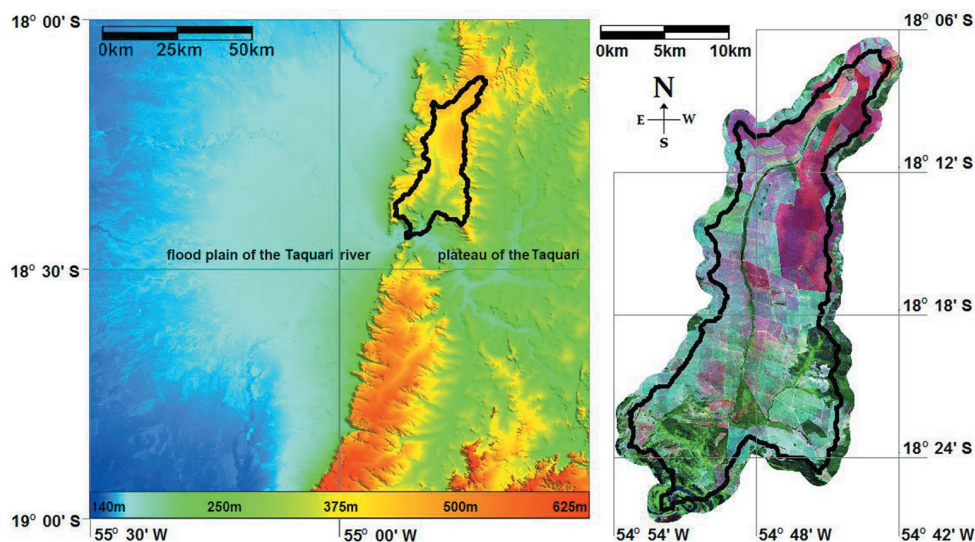
Figure 2 - Location of the Córrego do Veado sub-basin, altimetric variation of SRTM data, and enlargement (on the right) upon a GeoCover circa 2000 mosaic

The relief of the area under study presents medium height hills with convex peaks and some stretches of wide-peaked hills, with valleys showing average depth. In transitions between geologic structures, small escarpments or topographic ruptures occur, and relief dissection is more pronounced. (GALDINO et al., 2006, p.50).

MATERIALS

The SRTM data mosaic made available by the *Empresa Brasileira de Pesquisa Agropecuária Monitoramento por Satélite* (EMBRAPA) (MIRANDA, 2005), topographic sheet SE-21-Z-B was employed to model the relief forms from the sub-basin, using four refined DEMs. Analysis of the spatial distribution of results was performed based on tile S-21-15_2000 of the GeoCover circa 2000 ETM+/Landsat mosaic, available at https://zulu.ssc.nasa.gov/, and on DigitalGlobe images obtained by the QuickBird II sensor in August 2008, available in Google Earth (GOOGLE, 2010).

The software Idrisi (EASTMAN, 2006) was used to process and manipulate SRTM data. The software Surface (GOLDEN SOFTWARE, 2009) was used to provide geostatistical analysis and interpolation of DEMs. The software USLE-2d (DESMET; GOVERS, 1996a) has employed to correct false depressions resulting from the interpolation process, in order to adjust the DEMs to derive hydrologic variables.

METHODOLOGY

DEMs refined from SRTM data were interpolated through kriging (OLIVER: WEBSTER, 1990) in accordance with the method used to select geostatistical coefficients to refine SRTM data (VALERIANO, 2008). In preparation for the interpolation process, the SRTM mosaic tile was cut out with a rectangular mask, the sides of it were 1 km away from the sub-basin borders. SRTM data

were converted to vector points through the RASTERVECTOR tool (IDRISI software package), passing from a matrix to a vector data structure, and afterwards it was exported in an ASCII file containing geographic coordinates (longitude and latitude) and elevation (altitude) of the points.

The experimental semi-variogram (model = Gaussian; nugget effect = 0.001; semi variance scale = 0.055; range = 0.002) was modeled based on residues extracted by the removal of the trend contained in the ASCII file, as illustrated in figure 3, using the Surface application. The semi-variogram was then re-scaled (standardized semivariogram) considering maximum variance of data, in order to support a comparison between semi-variograms at different orders of magnitude (VALERIANO, 2008, p.12)
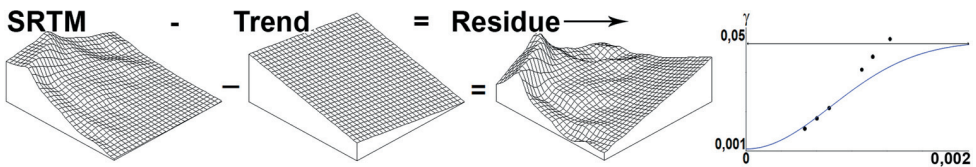

Figure 3 - Gaussian semivariogram adjusted to SRTM data residues for the Córrego do Veado sub-basin

Four DEMs were produced with grid spacing of 90m x 90m, 60m x 60m, 45m x 45m, and 30m x 30m, to enable the evaluation of the DEM influence to refine the calculation of *LS2d* variable. The tool Pit corrections at USLE-2d software was used to correct interpolated data and to generate hydrologically conditioned DEMs. Topographic variables $A_{(i,j)}$, $\theta_{(i,j)}$, $\phi_{(i,j)}$ were extracted from DEMs using USLE-2d software, and the routing across cells were estimated using the Flux Decomposition algorithm. Topographic variables extracted from DEMs were used to calculate the *LS2d* factor using equations shown on table 1.

Table 1 - Equations used to calculate the two-dimensional topographic factor *LS2d*

Equation	Formula	Author
1	$LS2d = L_{(i,j)} \times S_{(i,j)}$	(DESMET; GOVERS, 1996a)
2	$L_{(i,j)} = \dfrac{\left(A_{(i,j)} + D^2\right)^{m+1} - A_{(i,j)}^{m+1}}{\alpha^m \times D^{m+2} \times 22,1^m}$	(DESMET; GOVERS, 1996a)
3	$\alpha_{(i,j)} = \left|\sin\phi_{(i,j)}\right| + \left|\cos\phi_{(i,j)}\right|$	(DESMET; GOVERS, 1996a)
4	$m_{(i,j)} = \beta_{(i,j)} / \left(1 + \beta_{(i,j)}\right)$	(MCCOOL et al., 1989)
5	$\beta_{(i,j)} = \dfrac{\left(\sin\theta_{(i,j)}/0,0896\right)}{\left[3\left(\sin\theta_{(i,j)}\right)^{0,8} + 0,56\right]}$	(MCCOOL et al., 1989)
6	$S_{(i,j)} = -1,5 + \left(\dfrac{17}{1 + e^{\left[2,3 - 6,1\left(\sin\theta_{(i,j)}\right)\right]}}\right)$	(NEARING, 1997)

Equation 1 corresponds to the two-dimensional topographic factor $LS2d$ calculated on the product from factors $L_{(i,j)}$ and $S_{(i,j)}$ (slope length factor and slope steepness factor, respectively). Equation 2 corresponds to factor $L_{(i,j)}$, calculated from the contributing area $A_{(i,j)}$, of the spacing from grid D characteristic for the DEM, the slope length exponent m, and the flow width correction factor a for the DEM cell. Equation 3 is employed to calculate the correction factor α, based on the aspect angle of cell $\phi_{(i,j)}$. Equation 4 is used to calculate exponent m from the slope angle $\theta_{(i,j)}$, through the ratio $\beta_{(i,j)}$ of rill to interrill erosion estimated by Equation 5 (MCCOOL et al., 1989). Equation 6 corresponds to factor $S_{(i,j)}$, which is also calculated based on angle $\theta_{(i,j)}$ (NEARING, 1997).

Results obtained from different DEMs were compared by visual assessment of the spatial distribution of factor $LS2d$, plus analysis of value distributions and analysis of value regressions for factor $LS2d$, all calculated based on refined DEMs (60m x 60m, 45m x 45m, 30m x 30m), in comparison with values calculated based on the original DEM spacing (90m x 90m).

The visual assessment of the spatial distribution from results was made based on tile S-21-15_2000 of the GeoCover circa 2000 ETM+/Landsat mosaic, and on DigitalGlobe images obtained by sensor QuickBird II. The visual validation of results may lead to an abstraction condition. Thus the visual validation was guided by a comparison among resulting grids using a standard color palette generated for the visualization of $LS2d$ values in the sub-basin. The regression analysis was made based on 575 points sampled randomly within the limits of the area under study.

RESULTS AND DISCUSSION

An analysis of the results testifies the influence of refined DEM grid spacing to diagnose the erosion potential of the topographic features from the sub-basin. Observing graphs shown in figure 4, one sees that the refined DEM with grid spacing 30x30 presented the highest (97.3%) relative frequency of $LS2d$ values under 100, while the DEM with grid spacing 90x90 presented the highest (5.25%) relative frequency of $LS2d$ values above 100.
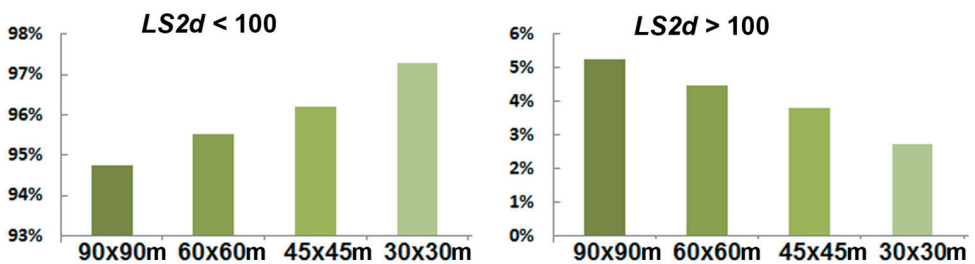

Figure 4 - Comparison of relative frequencies of values for the two-dimensional topographic factor LS2d calculated upon refined DEMs

Observing the measurements tending toward the center in the distribution of $LS2d$ values calculated based on the analyzed DEMs, we have noticed that refinement of SRTM data and the resulting reduction of grid spacing led to a reduction of average in the distribution of $LS2d$ values, as illustrated in the graph at figure 5.
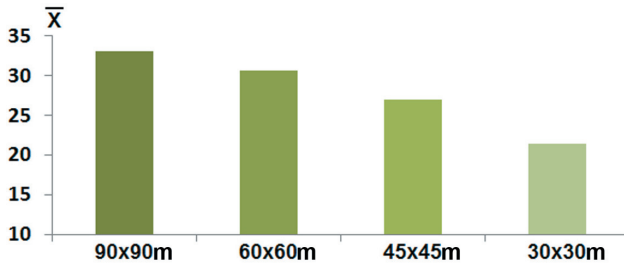
Figure 5 - Comparison of averages (X) of the two-dimensional topographic factor *LS2d* calculated upon grids generated from refined DEMs

Relative frequencies of *LS2d* values as presented in figure 4 could explain the differences observed in the values of averages represented in figure 5. One observes that the reduction in DEM grid spacing resulted in the decrease of the relative frequency from high values. Consequently, DEMs with reduced cell showed an increase in the relative frequencies of low *LS2d* values. The accumulated relative frequency enabled a continued assessment of how the distribution of *LS2d* values occurs. Figure 6 allows an analysis of distribution regarding the accumulated relative frequencies of *LS2d* values calculated on the four DEMs studied, for values ranging from 0 to 100.
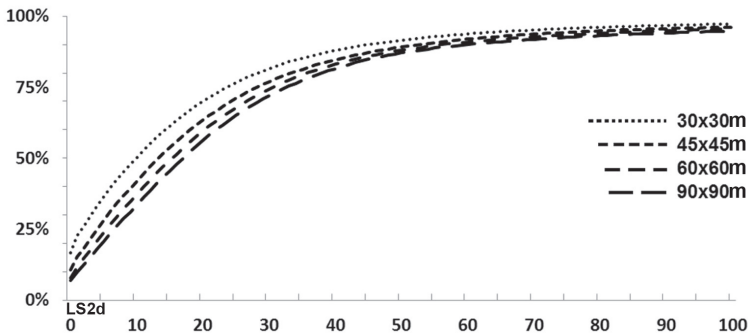

Figure 6 - Comparison of accumulated relative frequencies of the two-dimensional topographic factor LS2d values calculated upon refined DEMs

Analyzing figure 6 one observes that the larger the grid spacing from the DEM, the higher is the relative frequency of high values for *LS2d*. In other words, the refinement of SRTM data and the resulting reduction in DEM grid spacing helped to reduce the relative frequency of high values.

The spatial distribution of the *LS2d* factor as represented in figure 7, confirms the results found in the analysis of value distributions presented previously. Observing figure 7 one sees that the *LS2d* factor calculated on a 90x90 grid spacing DEM, presented higher values than those obtained from refined DEMs with reduced grid spacing.

The generation of grids with different spacings from the original DEM with a 90x90 spacing, introduces autocorrelation among models, thus biasing any quantitative validation, comparing such models with each other. However, tendency lines resulting of a regression analysis that was made on samples of *LS2d* grids, allowed us to present the behavior associated to punctual variation of values, as a function of DEM's grid spacing. Figure 8 shows the tendency of reduction in punctual values of *LS2d* as a function of the reduction in grid spacing.
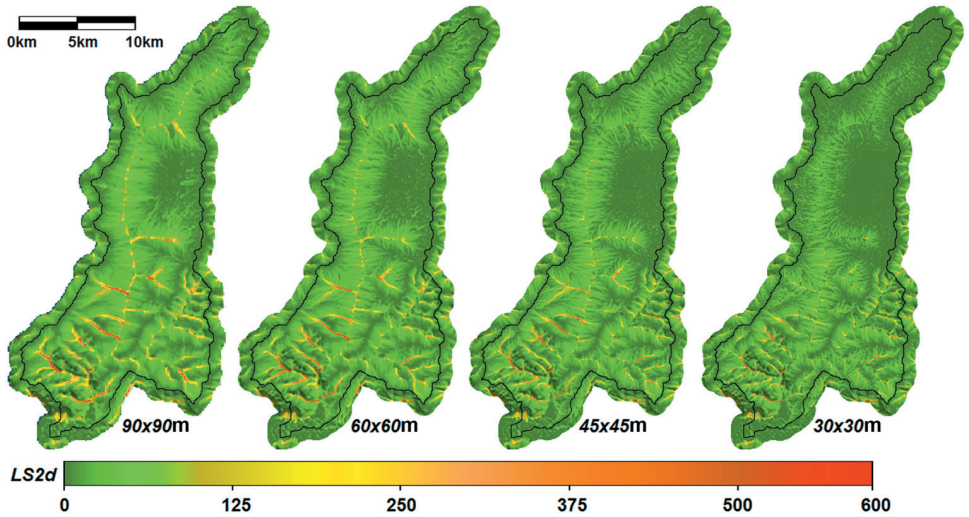
Figure 7 - Comparison of the spatial distributions of the two-dimensional topographic factor *LS2d* values calculated upon refined DEMs
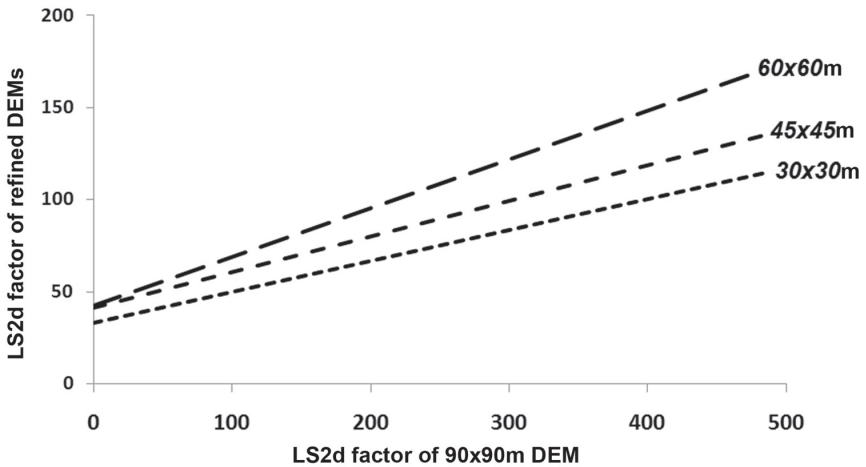

Figure 8 - Lines of tendency produced with the linear regression of the two-dimensional topographic factor *LS2d* values calculated upon refined DEMs

Although the refinement of SRTM data leads to a lower frequency of high *LS2d* values, we observed the occurrence of larger amplitudes in results obtained from DEMs with refined grid spacing. So the highest value of *LS2d* obtained by the DEM with grid spacing 90x90 was 2023, while at that one with the 30x30 DEM the top value was 2633.

We notice that the original spacing of SRTM data, of approximately 90x90, contributed to generalize areas with topographic features favorable to water erosion, as illustrated in Figure 9,

which was in benefit to identify areas with topographic characteristics most susceptible to erosion processes.
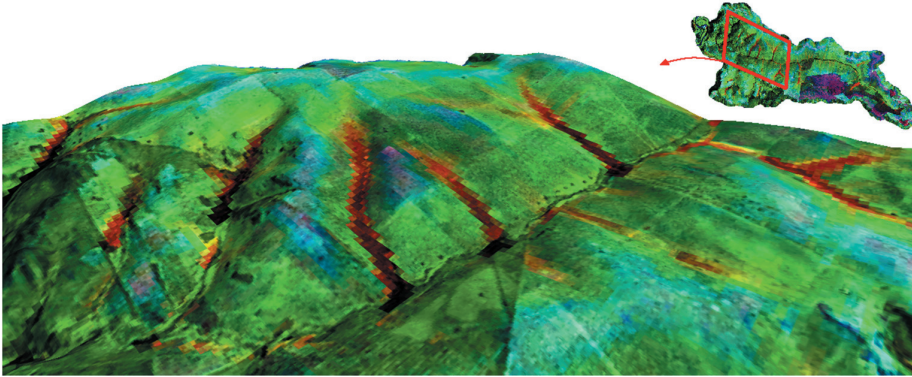

Figure 9 - Representation of areas susceptible to water erosion (in red,) using DEM and the GeoCover circa 2000 mosaic, superimposed by the two-dimensional topographic factor *LS2d*

Figure 9 presents, in shades of red, areas of waterflow concentration that are more susceptible to water erosion. Areas of flow concentration are found in regions characterized by concave curvature, while regions characterized by convex curvature show a greater divergence of flow, and low *LS2d* values in shades of blue.

We observed that the reduction in DEM grid spacing contributed to decrease the local average for *LS2d*. However, refined DEMs enable modeling of smaller areas, supporting the identification of converging flow zones and specific regions with high *LS2d* values.

Thus DEMs with reduced grid spacing, produced through the refinement of SRTM data, led to a decrease in the number of cells that indicate a higher potential for erosion. So the increase in DEM's grid spacing can benefit the general identification of areas with topographic characteristics more susceptible to erosion. Nevertheless the reduction in grid spacing allows a more detailed differentiation of areas where surface flow is concentrated, as illustrated in figure 10.
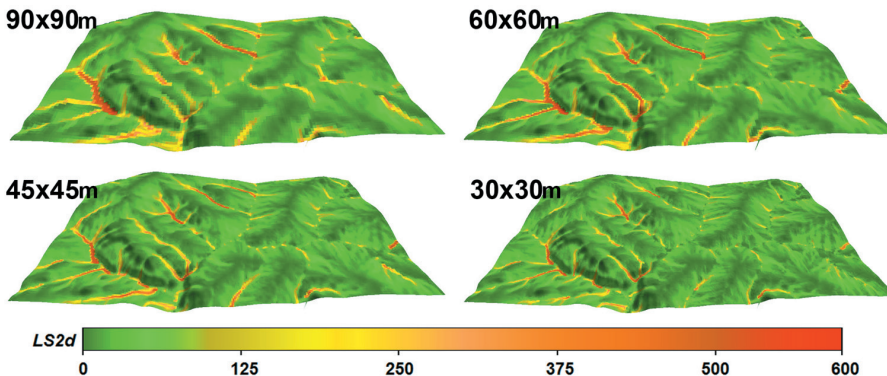

Figure 10 - Comparison among results of the two-dimensional topographic factors *LS2d* calculated for DEMs with different grid spacing

Figure 10 allows a visual comparison among results presented by grids with different spacing. Areas of flow concentration in regions with a concave curvature are shown in shades of red, while regions characterized by convex curvature and divergent flow are shown in shades of dark green. Results obtained from grids with larger spacing (90x90 and 60x60) evidence more clearly the areas of flow concentration or divergence, while results obtained from grids with smaller spacing (45x45 and 30x30) evidence more clearly the lines of surface flow, in light green shades.

The reduction in grid spacing by geo-statistical refinement of SRTM data should not be considered as an increase in DEM resolution. Resolution of topographic information such as it is characteristic of SRTM data, cannot be increased by an interpolation. However, the refinement of SRTM data allowed to reduce the DEM grid spacing using the topographic information's structure of variation, and then allowing the estimation of flow concentration patterns that are characteristic of the original spacing of SRTM data, using smaller cells, as illustrated by figure 11.
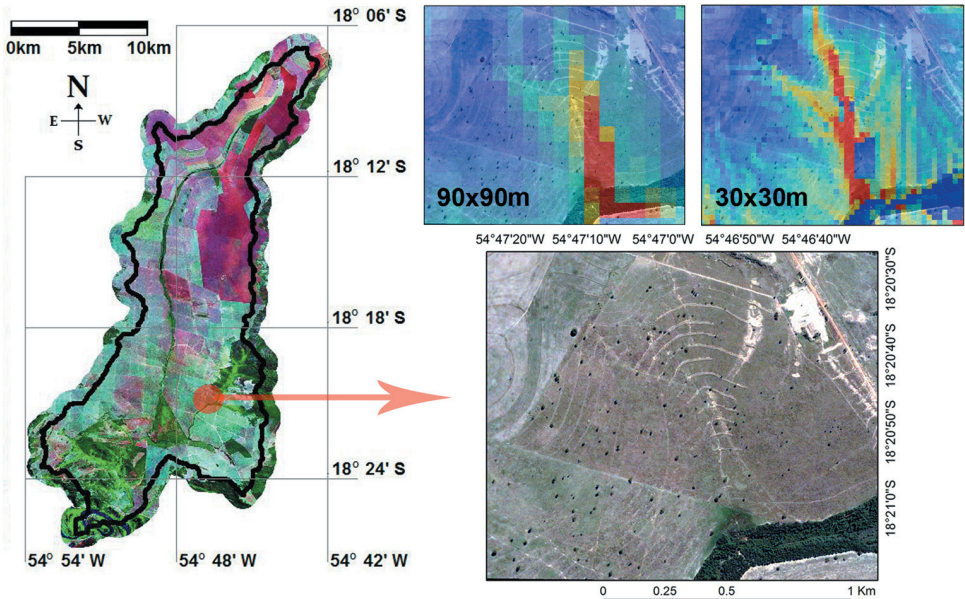

Figure 11 - Identification of areas more susceptible to water erosion (in red) by using DEMs with different grid spacing

The area of flow concentration illustrated in figure 11 presents contour lines as a practice for soil conservation and contention of erosion processes. The utilization of a grid with refined spacing helps to identify the lines of surface flow, in shades of yellow and red, according to comparison shown in figure 11. However, the interpolation process used to refine grids might originate cells with values of *LS2d* that are inconsistent with values in the neighborhood, according to cells in blue shades (low values of *LS2d*) illustrated at figure 11 in the region of flow convergence for grid 30x30.

The selection of the grid spacing to be used to generate a DEM used in the calculation of the *LS2d* factor must consider the scale in which erosion processes will be analyzed, as well as the accuracy of data to be used when crossing information to model water erosion in watersheds. Erosion modeling in large areas such as it is the case of BAT and BAP basins, may be helped with

the use of the original spacing of SRTM data (90m x 90m), while erosion modeling in sub-basins and in small water catchment areas may be aided with the refinement of SRTM data, as shown in figure 11.

The analysis of the influence of DEM grid spacing on the derivation of variables applied to erosion modeling is of key importance to improve soil loss estimation models. The establishment of databases with field-collected data containing size and location of erosion features can support absolute validation of the methodology, enabling comparisons between the resultant models and the erosion processes. In future studies it would be convenient to have a number of grids available with different spacings, and elevations determined independently for each individual cell and each grid, or alternatively, to start from a grid with good resolution and then interpolate other grids with larger spacing, in order to further detail the the analysis on the influence of grid spacing to the derivation of topographic variables required for erosion modeling.

CONCLUSIONS

The present study evaluated the influence from the refinement of a digital DEM on the calculation of a two-dimensional topographic factor *LS2d,* and implications resulting from a reduction in DEM grid spacing for the identification of areas with topographic characteristics most susceptible to erosion processes in a sub-basin. We conclude that DEM refinement and the resulting reduction of grid spacing change the distribution of *LS2d* (two-dimensional topographic factor) values, and therefore may influence in the identification of areas most susceptible to erosion. Thus, we point out that the refinement of SRTM data applied to model erosion processes in watersheds should take into consideration the influence of DEM grid spacing to determine the two-dimensional topographic factor *LS2d*.

REFERENCES

AGÊNCIA NACIONAL DE ÁGUAS (ANA). **Bases de dados georreferenciadas:** Ottobacias. Ottobacia_Nivel6.shp. Ministério do Meio Ambiente. Available at: <http://www.ana.gov.br/bibliotecavirtual/>. Accessed on January 23, 2010.

BOTELHO, R. G. M. Planejamento ambiental em microbacia hidrográfica. In: GUERRA, A. J. T.; SILVA, A. S.; BOTELHO, R. G. M. (Org.) **Erosão e conservação do solo**. Piracicaba: Ícone, 2009. 8, p. 269-300.

DESMET, P. J. J.; GOVERS, G. A GIS procedure for automatically calculating íthe USLE LS factor on topographically complex landscape units. **Journal of Soil and Water Conservation**, v. 51, p. 427-433, 1996a.

DESMET, P. J. J.; GOVERS, G. Comparison of routing systems for DEMs and their implications for predicting ephemeral gullies. **International Journal of Geographical Information Systems**, v. 10, n. 3, p. 311-331, 1996b.

EASTMAN, J. R**. IDRISI Andes**: guide to GIS and Image processing. Worcester: Clark University, 2006. 328 p.

FREEMAN, G. T. Calculating catchment area with divergent flow based on a regular grid. **Computers and Geosciences**, v. 17, n. 2, p. 413-422, 1991.

GALDINO, S.; PELLEGRIN, L. A. **Diagnóstico e Diretrizes do PCBAP relativos à erosão na Bacia do Alto Taquari**. Corumbá: EMBRAPA, 2003. 33p.

GALDINO, S.; RISSO, A.; SORIANO, B. M. A.; VIEIRA, L. M.; PADOVANI, C. R. Potencial erosivo da Bacia do Alto Taquari. In: GALDINO, S.; VIEIRA, L. M.; PELLEGRIN, L. A (Ed.). **Impactos ambientais e socioeconômicos na bacia do rio Taquari – Pantanal**. Corumbá: EMBRAPA, 2006. 5, p. 105-117.

GOLDEN SOFTWARE. **Surface Mapping System**. 9. Golden, CO: Golden Software Inc. 2009.

GOOGLE. **Google Earth**. 5. Mountain View, CA: Google Inc. 2010.

KINNEL, P. I. A. Alternative approaches for determining the USLE-M slope length factor for grid cells. **Soil Science Society of America Journal,** v. 69, p. 674-680, 2005.

MCCOOL, D. K.; FOSTER, G. R.; MUTCHLER, C. K.; MEYER, L. D. Revised slope length factor for the Universal Soil Loss Equation. **Transactions of the ASAE**, v. 32, p. 1571-1576, 1989.

MIRANDA, E. E. (Coord.). **Brasil em Relevo**. Campinas: Embrapa Monitoramento por Satélite, 2005. Available at: <http://www.relevobr.cnpm.embrapa.br>. Accessed on August 23, 2009.

MOORE, I. D.; BURCH, G. J. Physical basis of the length-slope factor in the Universal Soil Loss Equation. **Soil Science Society of America Journal**, v. 50, p. 1294-1298, 1986.

NEARING, M. A. A single, continuous function for slope steepness influence on soil loss. **Soil Science Society of America Journal,** v. 61, n. 3, p. 917-919, 1997.

O'CALLAGHAN, J. F.; MARK, D. M. The extraction of drainage networks from digital elevation data. **Computer Vision Graphics and Image Processing**, v. 28, p. 323-344, 1984.

OLIVER, M. A.; WEBSTER, R. Kriging: a method of interpolation for geographical information systems. **International Journal of Geographical Information Systems**, v. 4, n. 3, p. 313-332, 1990.

PIMENTEL, D.; HARVEY, C.; RESOSUDARMO, P.; SINCLAIR, K.; KURZ, D.; MCNAIR, M.; CRIST, S. SHPRITZ, L. FITTON, L. SAFFOURI, R. BLAIR, R. Environmental and economic costs of soil erosion and conservation benefits. **Science**, v. 267, p. 1117-1122, 1995.

QUINN, P. F.; BEVEN, K. J.; CHEVALLIER, P.; PLANCHON, O. The prediction of hillslope flow paths for distributed hydrological modeling using digital terrain models, **Hydrological Processes**, v.5, p.59-79, 1991.

TARBOTON, D. G. A new method for the determination of flow directions and upslope areas in grid digital elevation models, **Water Resources Research**, v.33, n.2, p.309-319, 1997.

VALERIANO, M. M. **TOPODATA**: Seleção de coeficientes geoestatísticos para o refinamento unificado de dados SRTM. São José dos Campos: INPE, 2008. 50 p.

VERSTRAETEN, G. Regional scale modeling of hillslope sediment delivery with SRTM elevation data. **Geomorphology,** v. 81, p. 128-140, 2006.

WISCHMEIER, W. H.; SMITH, D. D. **Predicting rainfall erosion losses**: a guide to conservation planning. Washington: USDA, 1978. 58p.

ZEVENBERGEN, L.W.; THORNE, C.R. Quantitative analysis of land surface topography, **Earth Surface Processes and Landforms**, v. 12, p. 47-56, 1987.

MOISÉS PEREIRA GALVÃO SALGADO

(Instituto Nacional de Pesquisas Espaciais / Divisão de Sensoriamento Remoto, Discente (Mestrado em Sensoriamento Remoto), Av. dos Astronautas, 1758 - Caixa Postal 515, CEP 12201-970 - São José dos Campos - SP, Brasil. E-mail: salgado@dsr.inpe.br)

ANTONIO ROBERTO FORMAGGIO

(Instituto Nacional de Pesquisas Espaciais / Divisão de Sensoriamento Remoto, Pesquisador Titular III, Av. dos Astronautas, 1758 - Caixa Postal 515, CEP 12201-970 - São José dos Campos - SP, Brasil. E-mail: formag@dsr.inpe.br)

BERNARDO FRIEDRICH THEODOR RUDORFF

(Instituto Nacional de Pesquisas Espaciais / Divisão de Sensoriamento Remoto, Pesquisador Titular III, Av. dos Astronautas, 1758 - Caixa Postal 515, CEP 12201-970 - São José dos Campos - SP, Brasil. E-mail: bernardo@dsr.inpe.br)